Supramolecular Magnetorheological Polymer Gels

B. Hu,[1] A. Fuchs,[1] S. Huseyin,[2] F. Gordaninejad,[2] C. Evrensel[2]

[1]*Department of Chemical Engineering, University of Nevada, Reno, 1664 N. Virginia Street, Reno, Nevada*
[2]*Department of Mechanical Engineering, University of Nevada, Reno, 1664 N. Virginia Street, Reno, Nevada*

Received 7 February 2005; accepted 8 September 2005
DOI 10.1002/app.23578
Published online in Wiley InterScience (www.interscience.wiley.com).

ABSTRACT: Novel magnetorheological fluids—supramolecular magnetorheological polymer gels (SMRPGs)— were investigated. Supramolecular polymer deposited on the surface of iron particles was suspended in the carrier fluids. The supramolecular network was obtained by metal coordination between terpyridine monomers and zinc ion. These SMRPGs had such advantages as controllable off-state viscosity, a reduced iron particle settling rate, and stability. The viscoelastic behavior of SMRPGs with small- and large-amplitude oscillatory shear was investigated using the amplitude and frequency sweep mode. The effects of strain amplitude, frequency, and magnetic field strength on the viscoelastic moduli were measured. The linear viscoelastic (LVE) strain range was obtained by the oscillation and static stress strain methods. The maximum LVE value was equal to the preyield strain point, 0.3%. Microstructural variation of SMRPG is proposed as an explanation of the rheological changes in the oscillation tests. The results of this research indicate that off–state viscosity and particle settling can be controlled by adjusting the concentration of supramolecular polymer gel. Dynamic yield stress significantly increased with an external magnetic field up to ~23,500 Pa under a magnetic flux density of 500 mT. J Appl Polym Sci 100: 2464–2479, 2006

Key words: supramolecular structures; rheology; gels

INTRODUCTION

In recent years magnetorheological fluids (MRFs) have attracted considerable attention because their mechanical and rheological properties can be electrically controlled. MRFs are magnetic suspensions, which have particles with high permeability dispersed in a viscous or viscoelastic nonmagnetizable carrier fluid. Without an external magnetic field, MRF behavior is similar to that of a Newtonian fluid.[1,2] When a magnetic field is applied, magnetic polarization is induced in each particle, and the resulting dipole–dipole interaction force between the particles leads to the formation parallel to the applied field of chain- or columnlike structures that restrict the flow of the fluid. As a result, the rheological properties of the material can be controlled by an externally applied magnetic field.

The MR effect was discovered by Rabinow in the late 1950s. However, research studies of MRFs and their applications began more recently, in the mid-1980s. The successful application of MR fluids to commercial uses first occurred in the mid-1990s. At present, MRFs can be used in a variety of applications, including engine mounts, shock absorbers, clutches, and seat dampers. Other applications are in exercise equipment and spherical optical lens polishing.[3]

A new generation of MRFs, known as magnetorheological polymer gels (MRPGs) and developed by Fuchs et al., are used in vibration control and damping devices.[4–6] These fluids contain partially crosslinked polymer gels that are synthesized using nonstoichiometric amounts of monomers. Two MRPGs have been developed[6]: hydrocarbon polyol polyurethane MRPG and silicone MRPG. Adjusting the ratio of resin to crosslinker and the percentage of diluents can control the off-state rheology of the system. Fuchs et al. also investigated the static shear yield stress, off-state viscosity, and sedimentation properties of these systems. These fluids have the advantages of being able to control off-state viscosity and to reduce the settling rate of the magnetic particles in the fluid. This behavior is possible because the polymer gel distributes itself between the carrier fluid and the surface of the magnetic particles. Polymerization may take place before or after the addition of the magnetic particles. With the latter precipitation of polymeric gel on the surface of the iron particles may result, which will improve the stability of the system.[4]

Generally, MRPGs have four components: iron particles 5–10 μm in diameter, carrier fluid, polymers dispersed in the system, and additives and dispersants. Iron particles exhibit rapid, nearly completely reversible formation of columnlike structures when an external magnetic field is applied (this is known as the on state). The carrier fluid is the medium in which all

Correspondence to: A. Fuchs (alan.fuchs@gmail.com).

the components are suspended. The additives provide stability to the mixture and surface protection, which extend the operating life of the MRPGs and the device. The stabilization and redispersion of the carbonyl iron particles in the carrier medium are attributed to the adsorption of polymer on the surface of the iron particles, thus sterically preventing the particles from aggregating.

From our research, we propose another novel magnetorheological system, supramolecular magnetorheological polymer gel (SMRPG), which are different from the previous generation of MRPGs. In SMRPGs, the polymer in MRPGs is replaced by a supramolecular polymer containing a noncovalent bond.[7] Supramolecular polymers are defined as polymeric arrays of monomeric units that are self-assembled by reversible and highly directional secondary interactions that include hydrogen bonds, metal bonds, π–π stacks, donor–acceptor associations, electrostatics, and hydrophilic–hydrophobic and van der Waals forces, resulting in polymeric properties in dilute and concentrated solutions as well as in bulk. In this study, supramolecular polymer gel is defined as the crosslinked system in the appropriate organic solvent in which a linear polymer is crosslinked by a side noncovalent bond. Self-assembly of polymeric supramolecules is a powerful tool to produce functional materials that combine several properties and respond to external conditions. Examples, including the hexagonal self-organization of conjugated conducting polymers and polarized luminescence in solid-state films of rodlike polymer obtained by removing hydrogen-bonded side chains from the aligned thermotropic smectic phase, are described by Olli et al.[8] They demonstrated that hierarchically structured materials may be obtained by applying different self-organization and recognition principles and directed assembly, which are the bases for the production of tunable nanoporous materials and smart membranes, the preparation of nano-objects, and the achievement of anisotropic properties such as proton conductivity. As a consequence of their polymeric nature, these materials, for example, can be spin-coated into thin films or used as a bulk system. By changing the polymeric constituent, the macroscopic properties of the material can be changed dramatically, for example, from rigid to elastic, from hydrophobic to hydrophilic, or from liquid to solid.

There are two general approaches to making these supramolecular polymers.[9] In one approach, noncovalent bonding occurs on the side chain of a polymer, thereby forming the crosslinked network of a supramolecular system and introducing new properties into the polymer system. In the other approach, the supramolecular polymer is formed by small molecules or oligomers between which noncovalent bonds such as hydrogen bonds between small molecules or oligomers are used for self assembly; therefore, an extended linear chain can be formed. However, in the second approach, the behavior of the materials is more like that of small molecules than of polymers.

The study of polymeric materials containing coordination bonding has recently become an important field in macromolecular chemistry. It has been recognized that incorporation of metal atoms into polymer chains may lead to improved physical properties. Self-assembly is a useful tool for creating supramolecular metal-containing polymeric structures. This approach helps to produce self-organized, functional materials whose properties complement those of purely organic systems.[10] Among the previously mentioned secondary interactions, metal–ligand bonds exhibit interaction that is both strong and directional, with the selection of metal ion and ligand dictating association.[11] In particular, terpyridine–metal is widely used as a building block in supramolecular systems. An interesting aspect of a supramolecular polymer is that the terpyridine–metal complex is reversible. This is a key factor in the design and application of smart and switchable materials. Applications of these materials will range from intelligent glues to self-repairing coatings. The reversible nature of the metal–ligand interaction was demonstrated by Chujo et al.[12,13] They synthesized metal induced gelation of polyoxazolines containing bipyridyl units. From their observation of a solid precipitate after the addition of a metal ion, they assumed that a supramolecular network had been formed. When they diluted the system in solvent, the solid swelled and then dissolved.

In principle, all traditional polymer architectures can be produced using supramolecular interactions as a connection between polymer chains of various sizes and compositions. For example, diblock copolymers of polystyrene and poly(ethylene oxide) were prepared utilizing a bisterpyridine ruthenium complex as the noncovalent interaction for the connection of the two blocks.[14] By introducing the terpyridine ligand at the chain end of different polymers of various lengths, a large number of building blocks for block copolymers could be obtained. Applying this strategy and using different transition-metal centers and counterions, the possibilities for assembling the supramolecular block copolymers were virtually unlimited. Using polymers with a terpyridine complex in the backbone is another approach to building supramolecular polymers. Stiff ditopic ligands and oligomers derived from terpyridines bridged by an alkyne spacer comprised of one to four ethynyl groups have been reported.[15] These polyalkynylene chains allow the very fast exchange of electrons between photoactive terminals. Polymers with a terpyridine unit in the side chain also have been investigated. Terpyridine molecules were incorporated into the polymer side chain. Usifer et al.[16] homopolymerized 4′-vinylterpyridine through free-rad-

ical polymerization and then copolymerized it with styrene. The addition of metal ions that can formulate a metal coordination bond with the side terpyridine attaching on a polymer backbone resulted in a crosslinked polymer–metal network. The corresponding metal complexes were formed with $CoCl_2$, $FeCl_2$, NiCl, and $CuCl_2$. All the resulting polymers were white powders with molecular weights of up to 60,000 g/mol.

Alternatively, hydrogen bonding has been used in a variety of supramolecular systems.[10] Pourcain et al. used the hydrogen bond between carboxylic acid and pyridines to self-assemble an extended chain. However, it is known that polar environments will compete with the desired hydrogen bond and eliminate its association. Therefore, a hydrogen-bonding supramolecular system is not appropriate when the carrier fluid is a highly polar organic solvent.

In this article, we describe our research on the synthesis of a Zn-coordinated terpyridine polymer containing multiple metal ligands per chain. Terpyridine ligands were used because of their outstanding complexing behavior. This coordination bond, formed by metal–ligand bonds, remains, even in polar solvents.[11] In the SMRPG system, supramolecular polymer is on the surface of the iron particles that are suspended in the carrier fluids. These SMRPGs should inherit all the previously mentioned advantages of MRPG, such as having controllable off-state viscosity, reducing the iron particle settling rate, and being stable. Our hypothesis is that supramolecular polymers will increase the durability of the material because of the reversibility of the noncovalent bond. The reversibility of the associating segment suggests that improvement in redispersion may be achieved. Meijer et al. suggested that supramolecular polymers might quickly adjust their topology in response to external mechanical forces.[17] Therefore, in a supramolecular magnetorheological polymer gel system, the noncovalent bond should reversibly break when applying external shear stress and recombine after removal of that stress; thus, it should increase the durability of the material, the lifetime of the fluid, and the redispersion property of the iron particles. In this research, the rheology properties under static and oscillatory shear, iron-settling behavior, redispersion, and durability of novel SMRPGs were investigated.

EXPERIMENTAL

Materials

The SMRPGs were made up of carbonyl iron particles, carrier fluid, supramolecular polymer, and additives. The carbonyl iron particles (ISP Technologies Inc., Grade-R-2430) were 99.5% pure iron, with an average diameter of about 5 μm, and were formed by thermal decomposition of iron pentacarbonyl, $Fe(CO)_5$. Each sample contained 81 wt % carbonyl iron particles. The carrier fluid is an organic polar solvent typically chosen on the basis of its viscosity, freezing and boiling points, and vapor pressure. The solvent used in this study was *N*-octyl-pyrrolidone (Aldrich Chemical Company, Inc.), which has a boiling point of 306°C, viscosity of 9 cp at 20°C, and a vapor pressure of less than 1.3 Pa at 20°C. Graphite particles SLA 1275 (Acheson Colloids Company) are the additives, 2–3 μm in diameter, used to improve particle stability. The supramolecule was formed from the network of Zn-coordinated terpyridine polymer by metal-induced self-assembly.

Synthesis of metal-induced supramolecular polymer gel

The synthesis of the metal–ligand supramolecular polymer was carried out in two steps. First, the polymer with the side terpyridine functional group was synthesized, and then the supramolecular network was formed by the addition of zinc acetate. Figure 1 describes the synthesis procedure. Poly(vinyl alcohol) (0.57 g, 0.19 mmol), with a molecular weight of 3000 and 13 mmol OH functional group, was added to a suspension of KOH (0.5 g, 8.93 mmol) in DMSO (20 mL). After stirring for 1 h at 60°C, 4′-chloro-2,2′:6′2″-terpyridine (0.5 g, 1.9 mmol) was added. The mixture was reacted at 60°C for 24 h, and then the mixture was poured into cold distilled water. The suspension was extracted with chloroform. The organic mixture was dried by removal of the solvent in vacuum. The residue was dissolved in methanol, and after evaporation of the methanol, the white solid obtained (0.86 g) was the polymer with the side terpyridine group.

A methanol solution of zinc acetate with a molarity equivalent to that of 4′-chloro-2,2′:6′2″-terpyridine was added to a methanol solution of synthesized polymer. The color immediately changed to yellow. As more metal ions were added, the viscosity of the solution increased. This solution was added to the carrier fluid, *N*-octyl-pyrrolidone, and heated at 70°C to evaporate the methanol and maintain the concentration of the solution at 5%. This system contained a supramolecular polymer based on nonstoichiometric ratios of the reactants, including poly(vinyl alcohol) and 4′-chloro-2,2′:6′2″-terpyridine. The crosslink ratio of a supramolecular network depends on the ratio of the hydroxyl group from poly(vinyl alcohol) to the terpyridine group.

Synthesis of SMRPGs

The 81 wt % carbonyl iron particles were added to the supramolecular polymer gel and mixed at a low shear rate (400 rpm) using a Servodyne Mixer (model 50003-

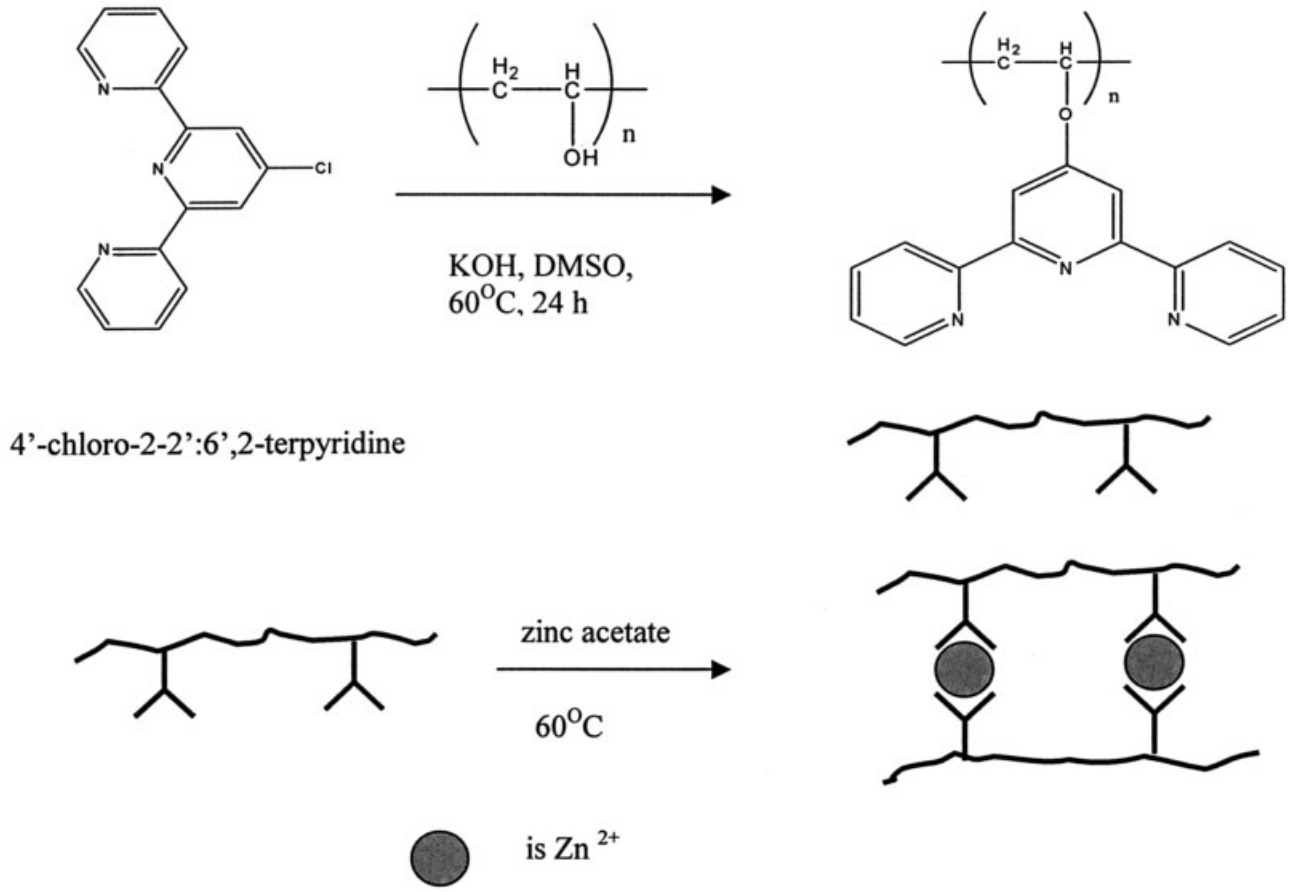

Figure 1 Synthesis of the metal-induced supramolecular polymer network.

30, Cole Parmer Instrument Company) for 30 min. The additives were mixed together and stirred thoroughly at 1200 rpm for 24 h at room temperature. Table I lists the components of the two SMRPGs with different supramolecular polymer weight ratios. Graphite particles were added to provide a stable suspension in a uniform, colloidal state in highly refined petroleum oil. This fluid was formulated to reduce friction and wear while preventing metal-to-metal contact and surface abrasion.

Methods and instrumentation

Magnetorheological rheometer

An Anton Paar Physica MER300 rheometer, operated in either a stress- or a strain-controllable mode, was used to measure the rheological property. A detailed description of this instrument was given previously.[18] This measurement system has three parts: the mechanical drive system, the electronics for data processing, and the corresponding software package. Unlike a conventional rheometer, the magnetic field applied to the material is generated by a built-in copper coil in which there are $N = 495$ turns and 1-mm-diameter coils generating the required magnetic field to the material. The magnetic strength across the plates is controlled by the rheometer software, which adjusts the electric current through the coil. The magnetic field is perpendicular to the gap filled with the material being investigated. The magnetic field (B) in the gap depends on the current in the coil and the material in the gap through which the flux flows. Two parallel disks 20 mm in diameter with a 1-mm gap between them were used for this study. Approximately 0.314 mL of sample was placed in this gap. By using this parallel plate arrangement, the torque transferred from the fluid to the rotor can be measured. In this research, this instrument was used to measure rheological parameters such as shear stress, shear strain, shear rate, and apparent viscosity of SMRPGs in the on- and off states. Oscillation was used to investigate the viscoelastic properties of SMRPGs under strain

TABLE I
List of SMRPG Components

Component	SMRPG 1	SMRPG 2
Iron particles (99.5% purity)	81%	81%
Carrier fluid (*N*-octyl-pyrilidone)	17.7%	16.8%
Supramolecular polymer (metal-induced complex network)	0.9%	1.8%
Colloidal graphite (SLA 1275)	0.4%	0.4%

amplitude sweep and frequency sweep. The effects of magnetic field strength, stain amplitude, and frequency on the storage and loss moduli also were investigated.

Particle settling

Sedimentation of iron particles caused by gravity causes severe problems with the operation of devices utilizing magnetic fluids. However, settling may be tolerated, to some extent, if the particles are easily redispersed. Sedimentation is a direct consequence of the greater density of iron particles than that of the carrier medium. When particle size is sufficiently small (<1 μm), gravitational force is opposed by a diffusion force associated with thermal Brownian motion. However, the yield stress of MR fluid decreases with a reduction in the size of the iron particles.

In this research, two methods were used to describe the settling behavior of SMRPGs. In one method the sedimentation behavior of particles in a carrier medium was measured by visual observation.[6] This was done by measuring the formation of a clear fluid layer on the surface of the MR fluid when a sample was permitted to settle for a time at room temperature. This layer was measured as a clear fluid volume fraction when the iron particles settled into the carrier fluid in a graduated glass cylinder. The change in clear fluid volume was measured as a function of time. The advantage of using this method is its simplicity. However, this method cannot be applied in opaque media, and much time is needed for a slowly sedimenting suspension.

Another method for measure the settling behavior was proposed by Gorodkin et al.[19] In this method, the settling velocity of iron particles is characterized by a sedimentation constant parameter. Sedimentation of the iron particles causes the upper layer of MR fluid to have a lower concentration of iron particles and therefore lower permeability. Using the method of Gorodkin et al.,[19] the MR fluid fills the tube such that the particles are at the top of the solenoid windings, and rotor rotation supplies a centrifugal force promoting sedimentation of the iron particles. These particles travel distance $\times$ leaving $-$ material within the solenoid. This sedimentation leads to reduced inductance in the solenoids, which is measured by an inductance meter. The rate of changing magnetic permeability of the MR fluid in the upper layer can be used as a measure of the sedimentation velocity of particles. The sedimentation rate of the iron particles in MR fluid is estimated with the sedimentation constant, S, which is the ratio of sedimentation velocity, u, to the acceleration of gravity, g.

$$S = u/g \tag{1}$$

where Svederg (1 Sb = 10^{-13} s) is the unit of measurement for S. As described in Gorodkin et al.,[19] the sedimentation constant, S, defined in eq. (1) is given by:

$$S = \frac{900\ln(1 + x/R_0)}{\pi^2 n^2 t} \tag{2}$$

where x is the distance traveled by particles for time t, R_0 is initial radius of the particles relative to the rotation center, and n is the rotation rate of the centrifuge shaft in revolutions per minute. The distance traveled by particles, x, is given by:

$$x = l\frac{L_{\max} - L}{L_{\max} - L_0} \tag{3}$$

where l is the length of the solenoid, $L_{\max}$ is solenoid inductance before onset of sedimentation, and L_0 is the inductance of a vacuum.

Redispersion measurement

The redispersibility, or remixing behavior, of MR fluid is an important issue. Magnetic particles settle because of the difference in density between the particles and the carrier fluid. However, these fluids can be used effectively in different devices such as dampers, if they redisperse quickly and completely.

It is believed that the hardness of the "cake" of carbonyl iron particles formed from the settling and agglomeration is an indication of the redispersibility. The harder the cake, the more difficult it is to redisperse the magnetic fluid. A redispersion method has been developed to quantitatively access this property.[20] To accelerate the settling process, the SMRPG samples were heated to 80°C for 24 h and then cooled to 25°C for 2 h. Thermal cycling was repeated three times. During thermal cycling the particles settled and formed a cake. The settled hardness after thermal cycling was measured using a micromechanical testing instrument (Perkin Elmer DMA-7e). The test was performed by increasing the force at a rate of 10 mN/min in order to depress the probe into the settled iron cake while measuring the displacement of the probe. Larger displacement of the probe indicated easier SMRPG redispersion. Figure 2 shows the schematic redispersibility measurement device.[20] To account for instrument error, measurements of the position are $\pm$50 nm, and measurements of the force are $\pm$0.001 mN.

RESULTS AND DISCUSSION

Uv–vis spectroscopy measurement

The combination of *N*-heterocyclic ligands and metal complexing segments with polymers, which has at-

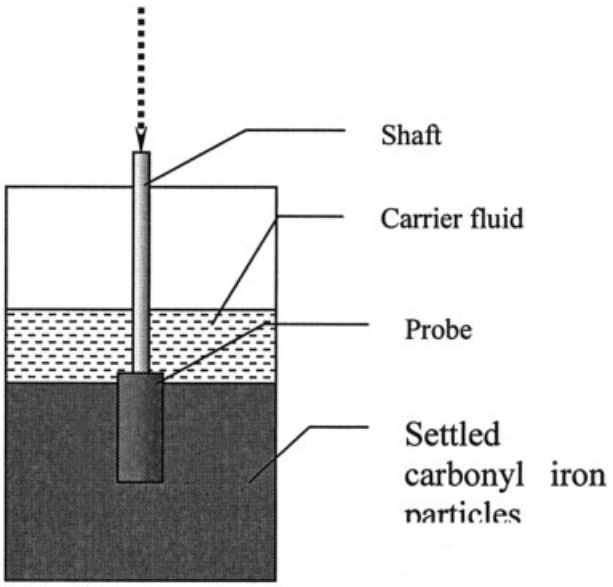

Figure 2 The redispersion measurement device.

tracted a great deal of interest recently, offers a new approach for organic–inorganic hybrid composites.[21] The addition of metal ions to terpyridine ligands leads to the formation of stable bis(terpyridine) metal complexes. The complexation can be easily monitored by UV–vis spectroscopy. Figure 3 shows the change in UV–vis absorption following the addition of zinc acetate to the terpyridine-containing polymer, which was synthesized from poly(vinyl alcohol) and 4′-chloro-2,2′:6′2″-terpyridine. The red shift of the π-π^* band at 205–210 and 280–290 mm, which is typical for the formation of terpyridine transition metal complexes, can be observed.[22]

Off-state apparent viscosity

Apparent viscosity is defined as the slope of the shear stress/shear rate curve. An important feature of SMRPGs is that off-state viscosity can be controlled by the concentration of the supramolecular polymer in the carrier fluid. A typical viscosity–shear rate curve for the supramolecular magnetorheological polymer gel without iron particles and additives (supramolecular polymer suspended in *N*-octyl-pyrrolidone in a 5% weight ratio) is also shown in Figure 4. The gel (without magnetic particles) remained Newtonian in this range of shear rates. This is because the presence of carrier fluid reduced the number of chain entanglements per unit volume.[23] The viscosity of the gel was about 36 cp. When iron particles were added, the material demonstrated non-Newtonian behavior and higher viscosity. One explanation for this proposed by

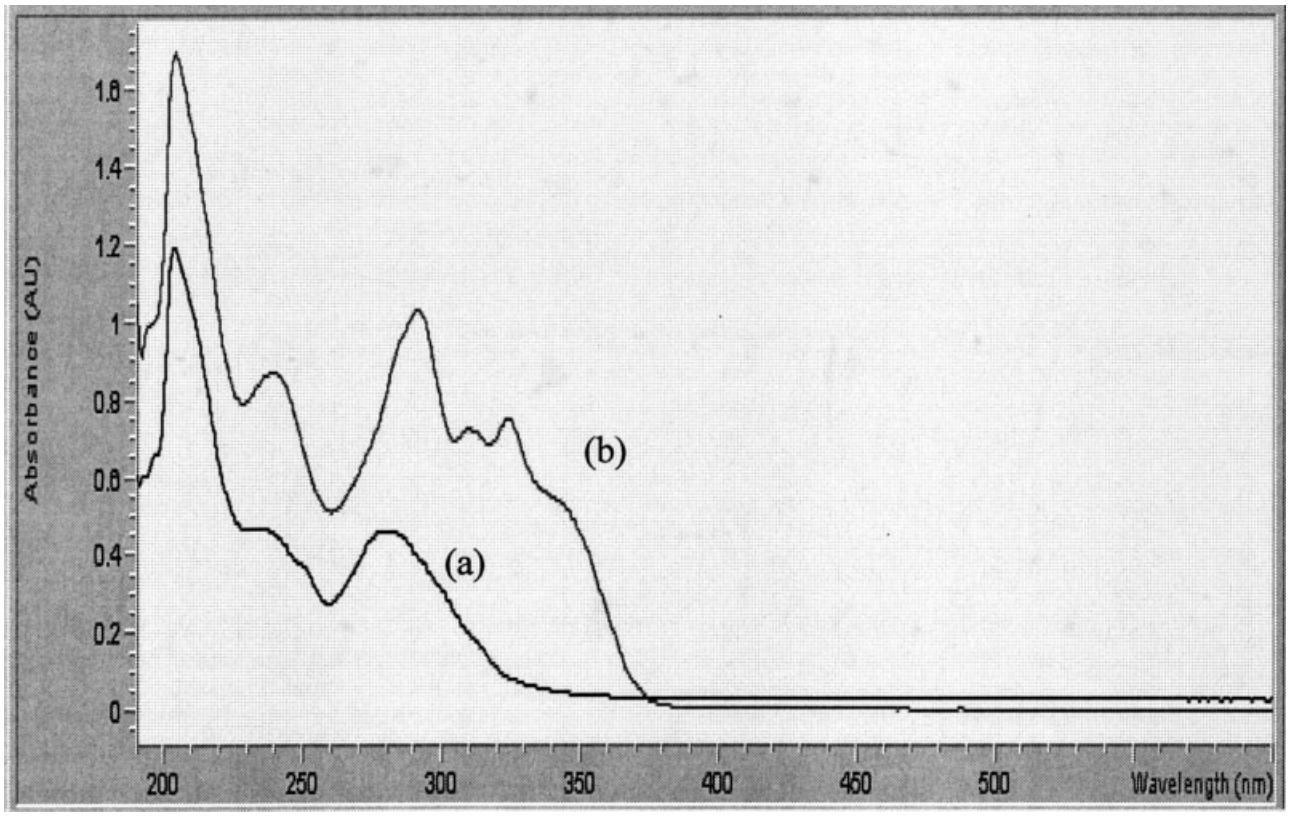

Figure 3 UV–vis spectra of (a) the uncomplexed polymer, (b) the polymer ion complex in methanol.

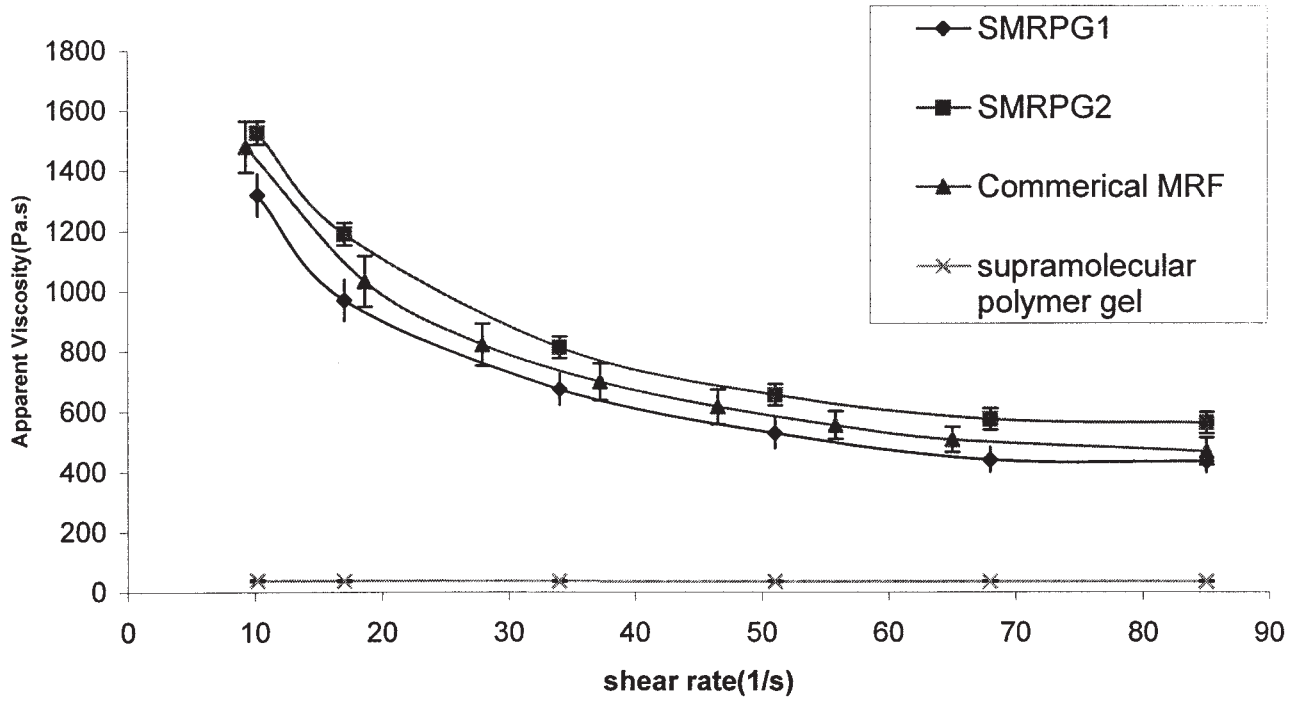

Figure 4 Apparent viscosity of various SMRPGs, a commerical MRF, and supramolecular magnetorheological polymer gel.

Frankel and Acrivos is that the increased viscosity from the addition of particulates resulted from energy dissipation in the thin liquid film between neighboring spheres as they moved past each other.[23] Viscosity also increased with the amount of supramolecular polymer in the carrier fluid, so that SMRPGs could be easily synthesized with tunable viscosities based on the application requirements.

Figure 4 shows a comparison of the apparent viscosity of SMRPGs with that of a commercially available MRF at room temperature in the off state. Apparent viscosity (η_{app}) decreased with increasing shear rate. This shear-thinning phenomenon resulted from the presence of micron-sized particles. At higher shear rates the apparent viscosity decreased, ultimately reaching a constant value. This shear-thinning phenomenon can be represented by the following equation[8]:

$$\eta_{app} \propto \gamma^{-\Delta} \tag{4}$$

where γ is the shear rate, and Δ is a constant that may vary slightly with different kinds of MR fluids. The experimental results showed that the range of Δ was about 0.54, 0.56, and 0.60 for SMRPG 1, SMRPG 2, and the commercial fluid, respectively.

Rheology in oscillatory shear

Oscillatory testing can be used to measure the behavior of viscoelastic materials, from low-viscosity liquid, pastes, gels, and polymer melts to elastomers and rigid solids. MR fluids change their rheological behavior almost immediately from a liquid to a semisolid state upon application of an external magnetic field. Many MR devices operate dynamically, and the MR fluid is under oscillatory shear loading. The linear viscoelastic (LVE) behavior of MR fluids in very small strains has been investigated by other researchers.[24–26] However, the nonlinear viscoelastic properties of MR fluid have not been extensively investigated.[23] Generally, there are two methods to investigate viscoelastic properties; one is amplitude sweep with variable strain amplitude and constant frequency, and the other is frequency sweep with variable frequency and constant strain amplitude. As long as the strain amplitude remains below the limiting value, γ_L, the G' curves show a constant plateau value, which means that the material is stable below this strain range. Many studies of MR fluids in the preyield region were based on linear viscoelastic theory. MR fluid behavior follows linear viscoelastic theory in the preyield regime.[24,25] According to this theory, the pre- and postyield behavior of an MR fluid can be determined with an oscillatory amplitude sweep test.

In the LVE range, MR fluid is subjected to a controlled oscillatory strain. The complex shear modulus can be expressed by:

$$G^* = \tau'/\gamma_0 + i^*\tau''/\gamma_0 = G' + iG'' \tag{5}$$

where

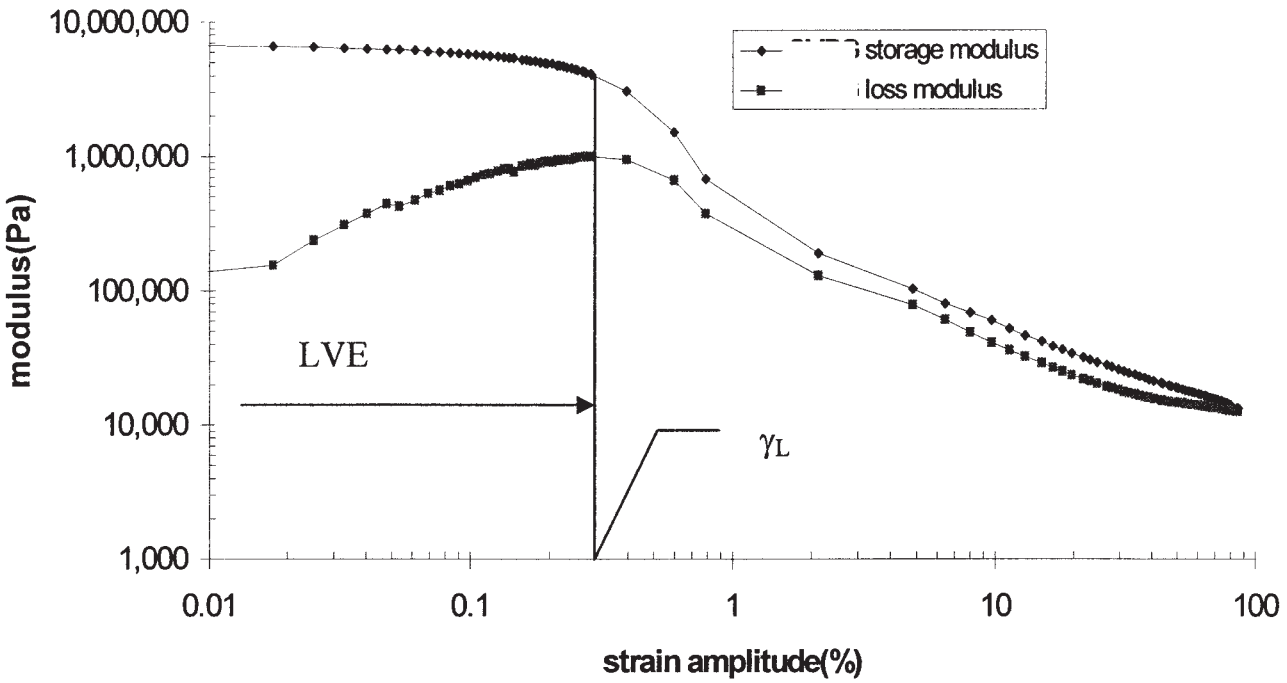

Figure 5 Storage modulus, G', and loss modulus, G'', as a function of strain amplitude, γ_0, at $B = 340$ mT, $T = 20°C$, and $\omega = 10$ rad/s.

$$G' = |G^*|\cos\delta = \tau_0\cos\delta/\gamma_0 \quad (6)$$

$$G'' = |G^*|\sin\delta = \tau_0\sin\delta/\gamma_0 \quad (7)$$

where δ is the loss angle, γ_0 is the amplitude of shear strain, and τ_0 is the amplitude of shear stress. G' is the storage modulus, which is a measure of the deformation energy stored in the sample during shear. After the load is removed, this energy is completely available and acts as the driving force for reformation. G'' is the loss modulus, which is a measure of the deformation energy lost during shear. This energy is either used up during the process by changing the sample structure or dissipated to the surroundings in the form of heat.

At strains higher than γ_L, the LVE is exceeded. At this point the sample structure changes. The shear stress response is no longer sinusoidal. The shear stress can be represented as a Fourier series of odd harmonics[27]:

$$\tau(t) = \sum_{n=1,odd}^{N} \tau_n \sin(n\omega t + \delta_n) \quad (8)$$

For a nonlinear response, all the dissipation is associated with the first harmonic only.[18] The first harmonic storage modulus and the loss modulus can be expressed as:

$$G' = \tau_1\cos\delta/\gamma_0 \quad (9)$$

$$G'' = \tau_1\sin\delta/\gamma_0 \quad (10)$$

Amplitude sweep

A strain amplitude sweep can be used to determine the limit of the linear viscoelastic range. Figure 5 shows the storage and loss moduli as a function of strain amplitude at $B = 340$ mT and $T = 20°C$, which was carried out with a strain amplitude ranging from 0.01% to 100% at a fixed frequency, $\omega = 10$ rad/s. The LVE can be determined from the G' curve because in the range of LVE, G' is almost a constant.[23] Figure 5 shows two typical regions separated by the critical strain amplitude, $\gamma_L = 0.30\%$. At very small strain amplitudes, less than γ_L, the storage modulus of SMRPG was insensitive to the strain amplitude. The region with strain amplitudes larger than γ_L is known as the nonlinear viscoelastic region. In this nonlinear region the storage modulus decreased significantly with increasing strain amplitude. An MR fluid exhibited linear viscoelastic behavior when it was subjected to preyield strain region. That means that when the applied strain amplitude was smaller than yield strain, γ_Y, the MR fluid exhibited linear viscoelastic behavior. It can be hypothesized that γ_Y should equal γ_L for an MR fluid. A shear method was used to measure γ_Y, and the results were compared with those from the oscillatory method.

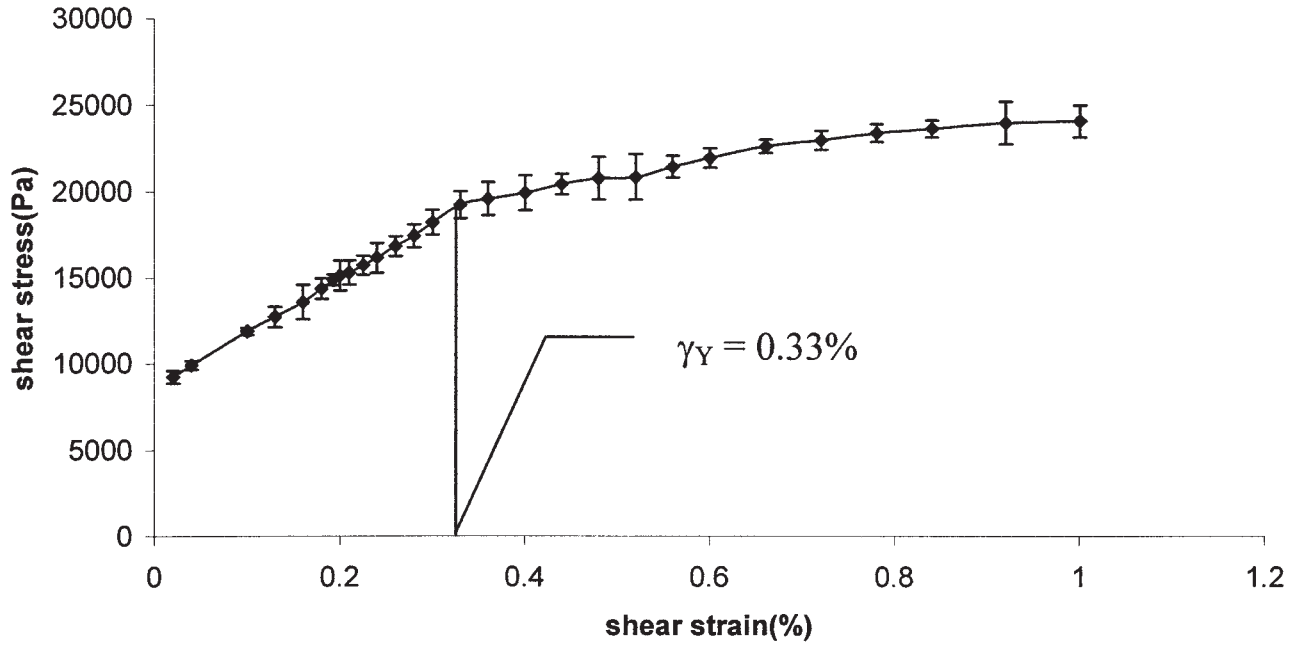

Figure 6 Shear stress dependence of shear strain with magnetic flux density of B = 340 mT at room temperature.

Figure 6 shows the stress dependence of shear strain with magnetic flux density at room temperature. The yield strain, γ_Y, shown in Figure 6, was ~0.33%, which was very close to the γ_L. In Figure 5, in the LVE range, the elastic behavior of SMRPG fluid dominated the viscous behavior; the structure exhibited rigidity be-

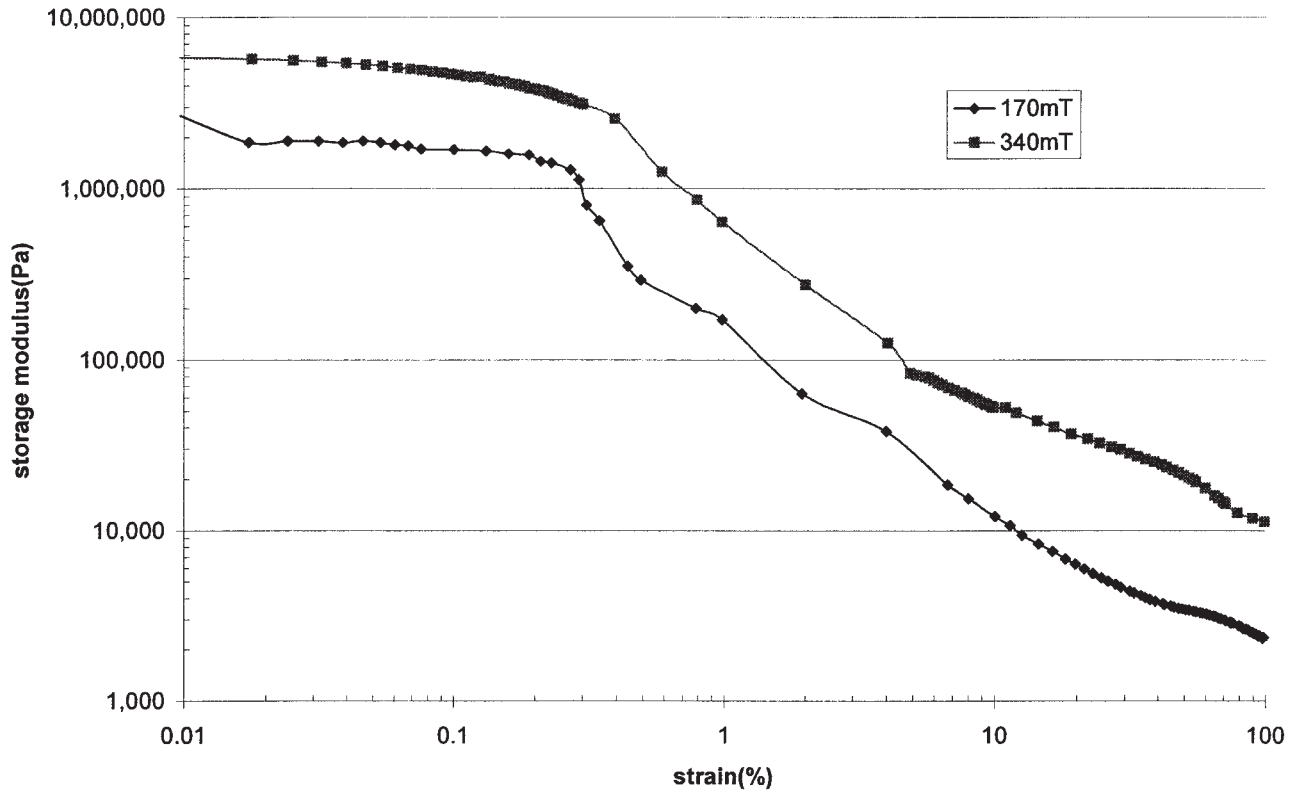

Figure 7 Storage modulus, G', as a function of strain amplitude, γ_0, at room temperature and ω = 10 rad/s with magnetic flux densities of 340 and 170 mT.

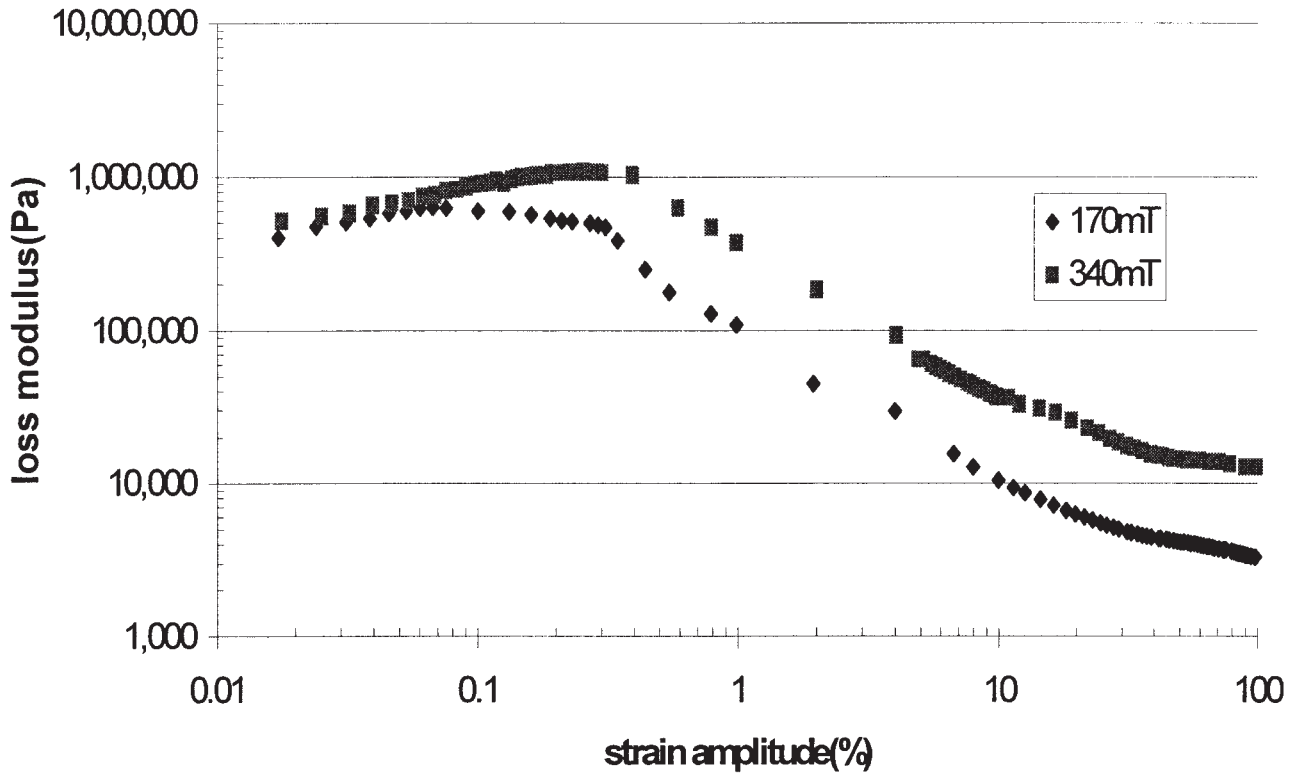

Figure 8 Storage modulus, G', as a function of strain amplitude, γ_0, at room temperature and $\omega = 10$ rad/s with magnetic flux densities of 340 and 170 mT.

cause G' was much higher than G″. The material behaved like a viscoelastic solid. This was expected because in the preyield range, the iron chains or columns that were induced by the external magnetic field had high stiffness. In the nonlinear range, the value of G' was just slightly higher than G″ because the viscous component increased significantly compared to that in the LVE region. The chains or column structures were irreversibly changed. The material behavior was intermediate between the elastic solid and the viscous liquid.

The dynamic viscoelastic behavior also was strongly dependent on magnetic field strength. Both the storage and loss moduli increased dramatically with an increase in the applied magnetic field strength, as shown in Figures 7 and 8. As can be seen in Figure 8, the loss modulus first increased slightly and then reached its maximum value before decreasing with increasing strain amplitude. The maximum occurred at γ_L, which means the energy loss of SMRPG increased with strain amplitude in the LVE range and decreased with strain in the non-LVE range.

Frequency sweep

1. *Linear viscoelastic region:* The critical strain amplitude, γ_L, of SMRPG was about 0.3% at an applied magnetic field strength of 340 mT. In this region ($\gamma < \gamma_L$), the storage modulus was approximately constant. In this section, the applied strain amplitude was fixed at 0.05%, and the oscillatory driving frequency was swept from 1 to 628 rad/s with the applied magnetic flux density of 340 mT. The storage and loss moduli for this material are shown in Figure 9. It can be seen that the storage modulus was independent of frequency, whereas the loss modulus decreased slightly with frequency. The storage modulus was much higher than the loss modulus within the frequency range. SMRPG exhibited a predominantly elastic response in the frequency range of 1–628 rad/s.
2. *Nonlinear viscoelastic region:* In this section, a constant strain amplitude of 5%, much larger than γ_L, was applied, and the driving frequency was swept from 1 to 1000 rad/s. Figure 10 shows the frequency (ω) dependence of G' and G″ at a constant strain amplitude of 5% and an applied magnetic field of 340 mT.

It can be seen that at low frequency, less than ω_p (defined as the frequency at which the storage modulus begins to decrease), the storage modulus remained constant until a critical frequency was reached; then, it began to decrease with an increase in frequency until

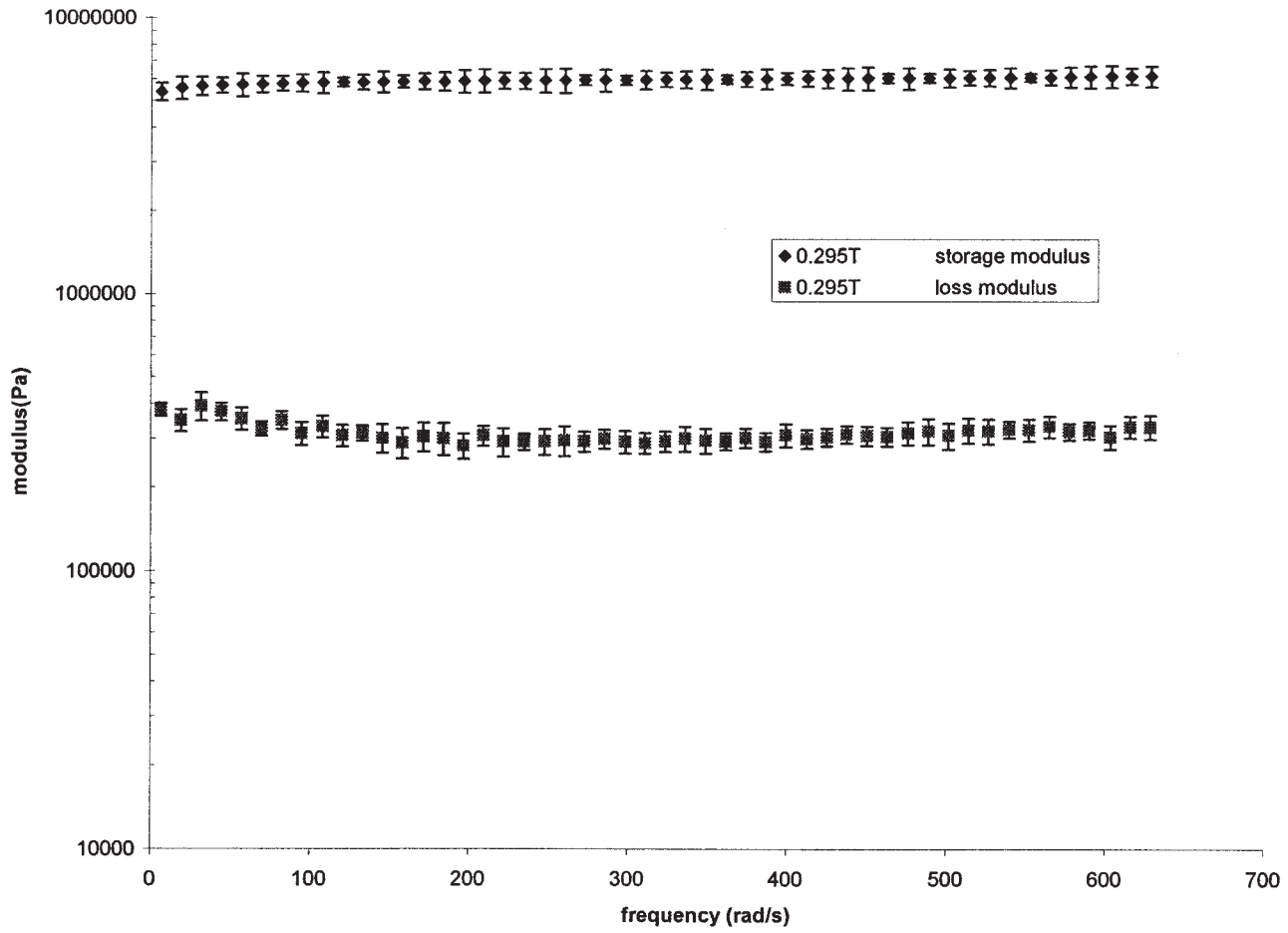

Figure 9 Dependence on frequency of loss and storage modulus, for SMRPG.

it reached its minimum value, frequency ω_m (defined as the frequency at which the storage modulus reaches its minimum value). Further increases in frequency led to an increase in the storage modulus. The loss modulus was nearly constant over this frequency range.

This interesting experimental result can be explained by the microstructural variation of MR fluids under an external magnetic field and at different frequencies.[21] MR fluids form chains, clusters, or columns under a magnetic field. At low frequencies, less than ω_p, the microstructure of the chains, clusters, and columns remains fairly constant because the shear rate ($\gamma_0\ \omega$) is very small. G', which characterizes the elastic component of the material, does not change as long as the microstructure remains constant. With further increases in the frequency, $\omega > \omega$p, some of the chains or clusters will be broken because of the high shear rate, which will decrease the elastic component. Therefore, G' decreases with an increase in frequency. When the frequency increases beyond ω_m, the value of G' increases with frequency. The reason for this behavior is that when frequency increases to ω_m, all the particle chains and clusters are irreversibly destroyed, and the iron particles distribute randomly in the on state. This microstructure is similar to that of the off state. Consequently, we measured the G' for the off-state SMRPG over the frequency sweep shown in Figure 11, where it can be seen that the G' for the off-state SMRPG increased with frequency in the range used in this experiment. Therefore, further increases in shear frequency would not cause any additional decreases in G'; in fact, it would increase it when the frequency was higher than $\omega_{\mathrm{m.}}$

Particle settling

Figure 12 shows the settling behavior of several SMRPGs compared to that of MR fluid without supramolecular polymer. A larger volume fraction indicates greater settling. It can be seen that the MR fluid, which only included carrier fluid and iron particles (without supramolecular polymer), had the greatest settling rate. When 1% supramolecular polymer was added, the settling rate decreased significantly. A possible explanation for this behavior is that a supramolecular network that could provided steric stabilization formed on the surface of the iron particles and in the

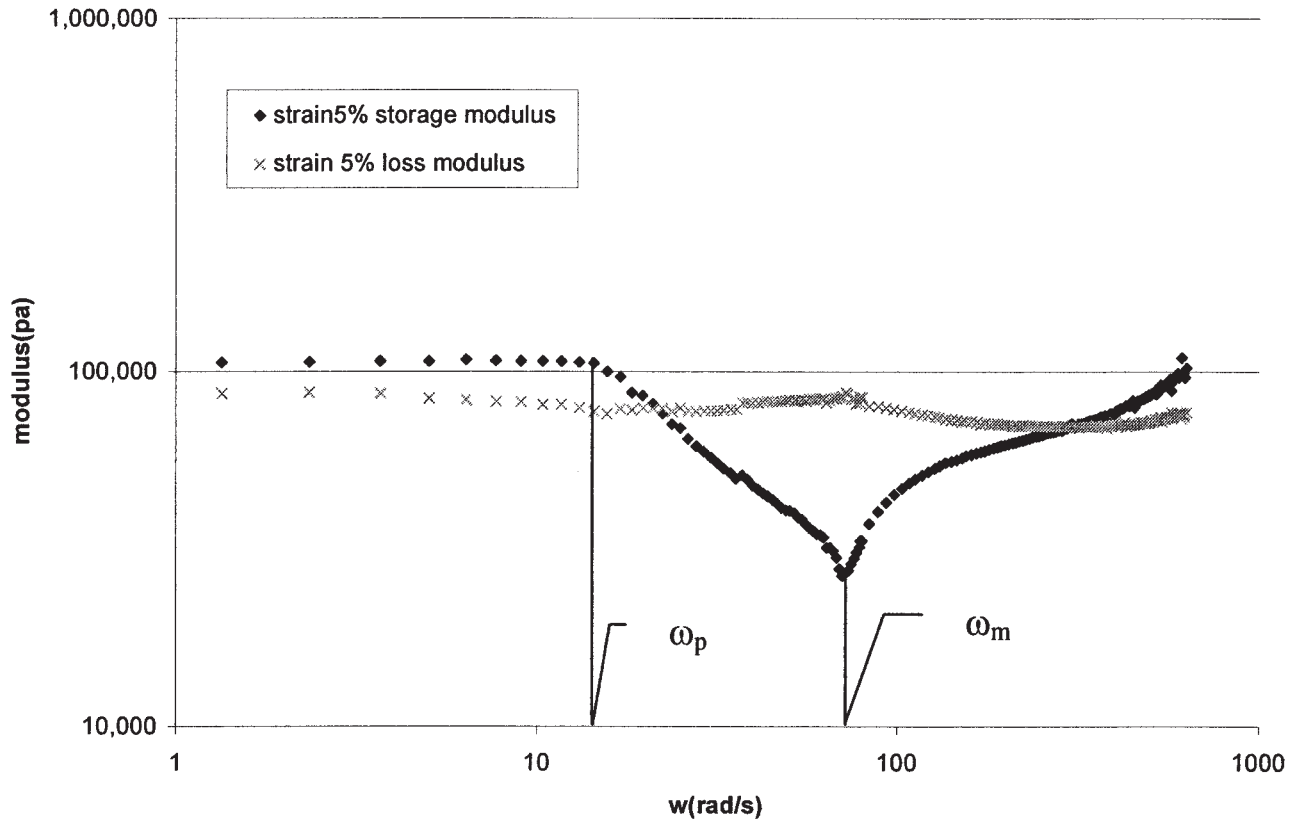

Figure 10 Storage and loss modulus as a function of frequency sweep.

region between iron particles. This was achieved by polymer molecules adsorbing or attaching to the surface of the magnetic particles, and depletion stabilization, a result of the molecules being in free solution, preventing the settling of iron particles. A comparison of the curves of the SMRPG and the SMRPG with graphite particles indicated that graphite particles also reduced the settling of iron particles. Two reasons may explain this behavior: the high viscosity of the SMRPG with graphite particles caused reduced settling, or the particles of graphite between the iron particles were to prevent them from agglomerating. In comparing the settling curves of SMRPG 1 and SMRPG 2, it can be seen that the increase in the supramolecular polymer could also reduce the settling behavior.

Figure 13 shows the curves of the settling velocities of the SMRPGs and MRF, generated by measuring the sedimentation constant. The measured results were consistent with those shown in Figure 12. The MRF had the greatest settling velocity and the SMRPG without additives the second greatest. The SMRPG with graphite particles (1.8% supramolecular polymer, 0.4% graphite particles) had the smallest sedimentation velocity. The curves shown in Figure 13 correspond to the slope of the corresponding curves of Figure 12 because the curves in the latter describe the change in position of the iron particles with time, so that the slopes of these curves indicate the settling velocity of iron particles, whereas the former shows the average velocity of settling. Consequently, the results using these two methods were consistent.

Dynamic shear yield stress

Changed rheological behavior resulted from the polarization induced in the iron particles by application of an external magnetic field. These induced dipoles caused the particles to align "head to tail" in chains and form columnar structures parallel to the applied field.[28] These chainlike structures hindered the flow of the fluid, thereby increasing the apparent viscosity of the suspension. The force needed to yield these chainlike structures increased with the applied magnetic field, resulting in field-dependent yield stress. Thus, the behavior of this type of controllable fluid in the postyield region is often represented as a Bingham plastic having variable yield strength, as follows:

$$\tau = \tau_y + \eta\gamma,\ \tau \geq \tau_y \tag{11}$$

where τ is the total shear stress, τ_y is the field-controllable shear yield stress, η is the plastic viscosity of the MR fluid, and γ is the shear strain rate. When the

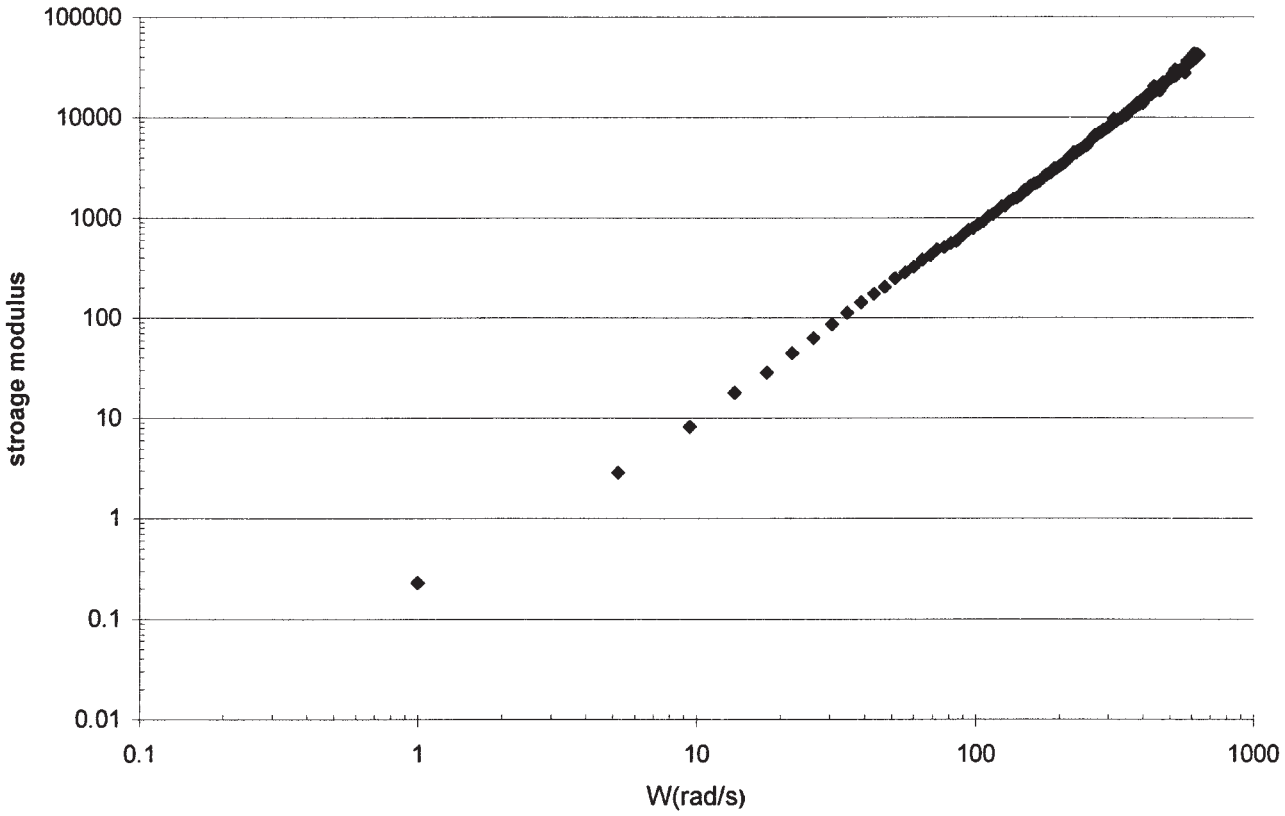

Figure 11 Storage as a function of frequency sweep for SMPG at off-state (0 *T*).

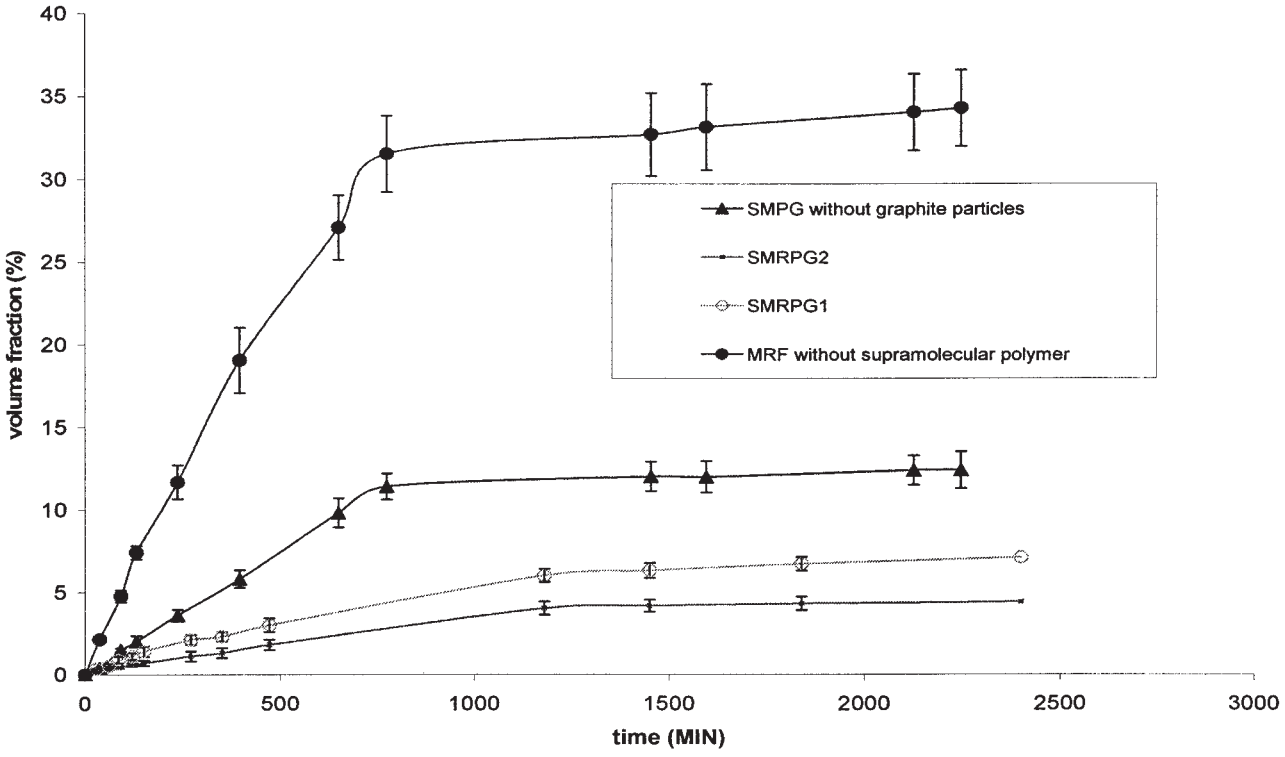

Figure 12 Settling curve of various SMRPGs and MRF without supramolecular polymer.

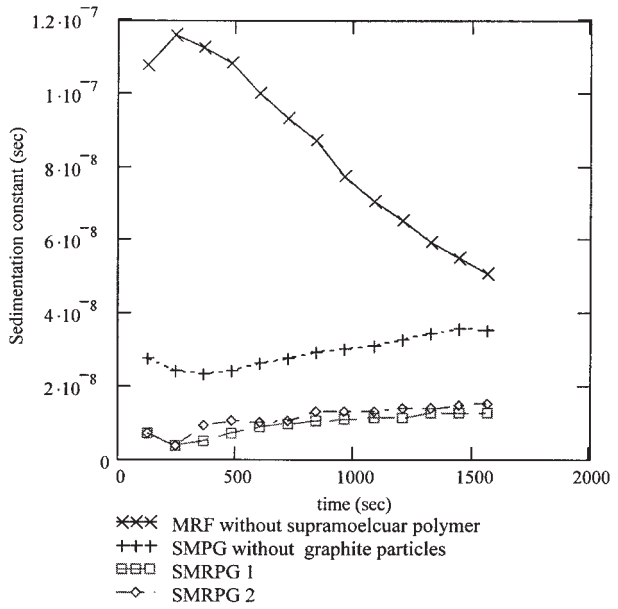

Figure 13 Settling velocity of SMRPGs and MRF without supramolecular polymer.

applied shear stress was less than the controllable shear yield stress, the SMRPGs behaved like viscoelastic solids. The relation between shear stress and shear strain is illustrated by eq. (12)

$$\tau = G\gamma \tag{12}$$

where G is the complex material modulus and γ is the shear strain. It has been observed that the complex modulus is also field dependent.[29]

An empirical model of yield stress for any MR fluids under an external magnetic field with a certain concentration of magnetic particles in MR fluids was found[28]:

$$\tau_y = C \times 271700 \times \phi^{1.5239} \times \tanh(H \times 10^{-6} \times 6.33) \tag{13}$$

where yield stress is represented in pascals, H is Am/m, and C is a constant that depends on carrier fluids: 1.0 for hydrocarbon oil, 1.16 for water, and 0.95 for silicone oil.

The effect of the applied magnetic field on the shear yield stress of the SMRPG was investigated using an MR rheometer. The shear stress versus strain rates with different applied magnetic flux densities for the MRPG are shown in Figure 14. It can be seen that dynamic shear stress was almost a linear function of shear strain rate, which can be expressed by the Bingham equation. Dynamic shear yield stress can be obtained by extrapolating shear stress data back to a zero strain rate. The plastic viscosity is the slope of the curve. Figure 14 shows the shear stress increased dramatically with applied magnetic flux density, whereas plastic viscosity was not significantly affected. For example, at a low magnetic flux density of 115 mT, dynamic yield shear stress was about 2400 Pa, whereas it was 23,500 Pa with a density of 500 mT. The yield stress increased about 9 times when the magnetic field strength increased 3.7 times, from 115–500 mT.

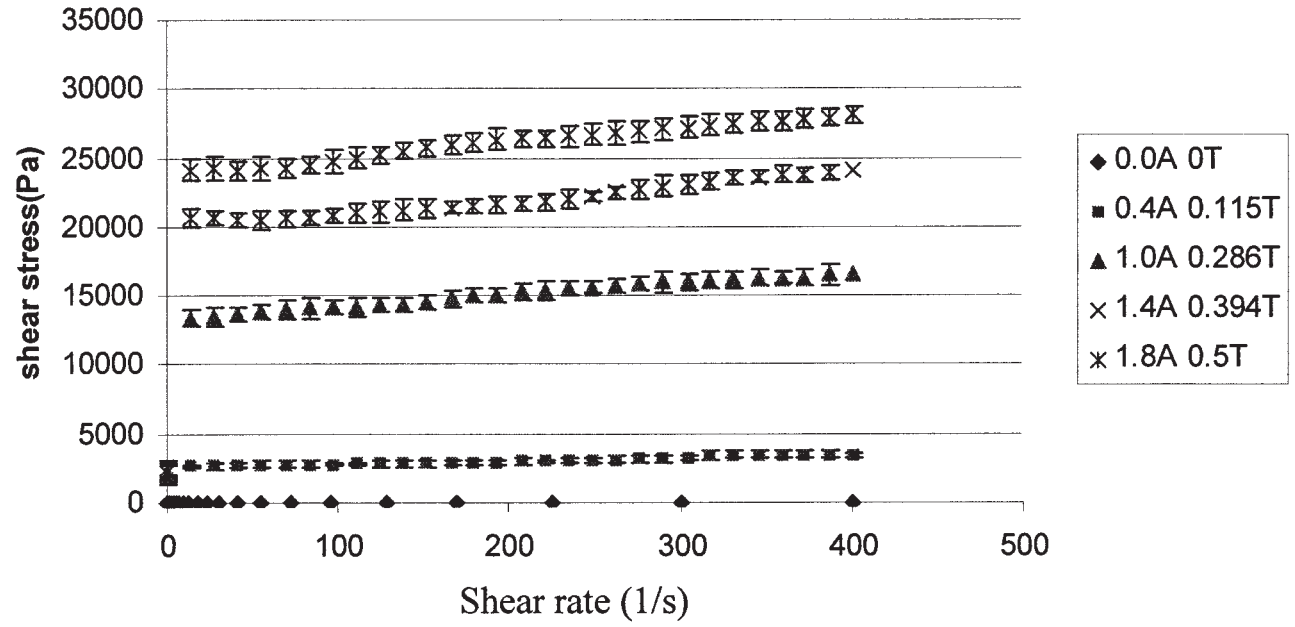

Figure 14 Dynamic shear stress versus shear strain rate with different values of applied magnetic field strength for SMRPG 1.

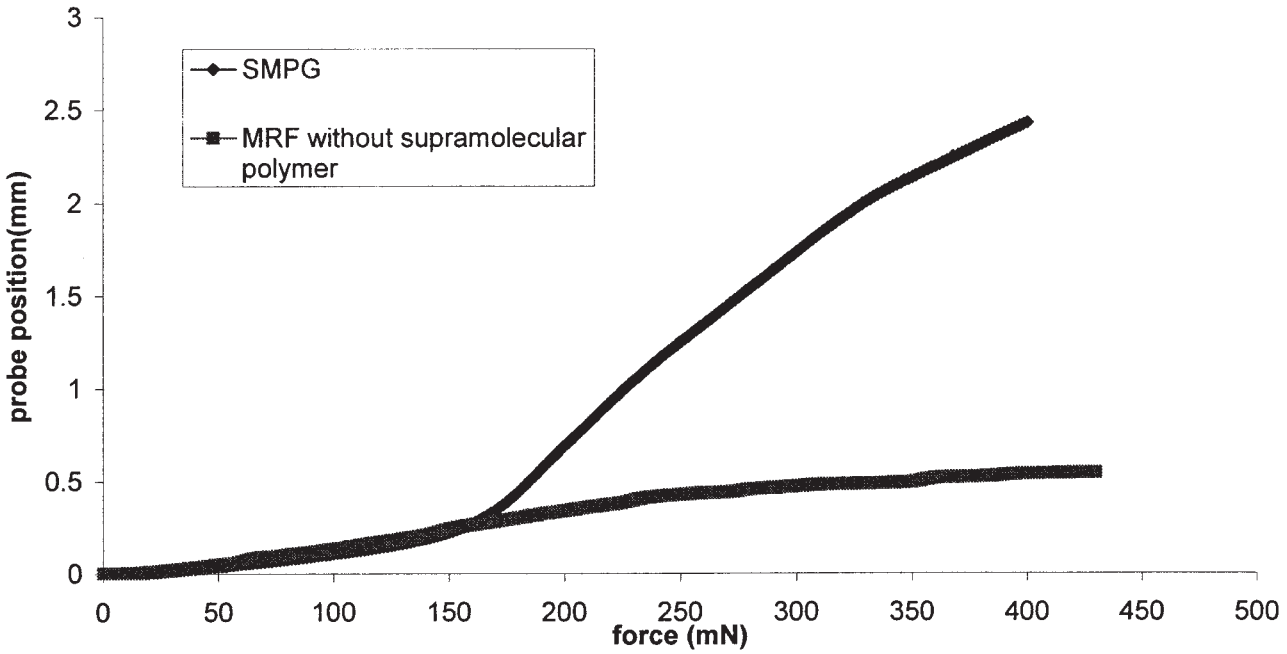

Figure 15 Redispersion of SMPG and MR fluid without supramolecular polymer.

Particle redispersion

Agglomeration results from the attractive van der Waals forces, which occurs when particles approach one another. A suspension of solid particles in a liquid has very high surface energy because there are individual particles, which have high surface areas. Therefore, processes accompanied by decreasing surface energy, such as the aggregation of particles, occur easily in these systems. To prevent agglomeration and to stabilize the MR fluid, iron particles had to be stabilized through forces of repulsion. Supramolecular polymer gels can provide polymeric stabilization including steric and depletion stabilization. In a sterically stabilized system, each iron particle is coated with physically or chemically adsorbed surface layers that hinder the particles from approaching each other at distances at which van der Waals forces would dominate. The thickness of the adsorbed layer is determined by the length of the polymer chain. Long polymer chains in solution can assume numerous configurations, resulting in repulsion between particles. In depletion stabilization, the close approach of iron particles must be accompanied by mixing of the polymer molecules with the carrier fluid in the interparticle regions and by driving the polymer molecules out of these interparticle regions. Work must be done to make the polymer molecules leave the interparticle region. This corresponds to a repulsion force between the particles.

Probe displacement for an applied force was used as the measure of dispersibility (Fig. 2). To investigate how supramolecular polymer affects redispersibility, the redispersion behavior of an MRF sample that contained only carrier fluid (*N*-octyl-pyrrolidone) and iron particles in a ratio of 19:81 (w/w) also was studied. The SMRPG sample contained a 1% concentration of supramolecular polymer. In Figure 15, it can be seen that the probe position for the MRF had greater values than that for SMRPG, which means the hardness of the settled iron particle cake for the MRF was higher than that of the SMRPG; thus, it was easier to redisperse SMRPG than to redisperse MR fluid. We speculate that this improved redispersibility resulted from the reversibility of the supramolecular bonds in the SMRPG.

Error analysis

The error measurement of each parameter was repeated three times. The error analysis used the student t distribution.[30]

$$Upper\ Limit = \bar{x} + \frac{(t_{\alpha/2})s}{\sqrt{n}} \tag{14}$$

$$Lower\ Limit = \bar{x} - \frac{(t_{\alpha/2})s}{\sqrt{n}} \tag{15}$$

where $\bar{x}$ is the mean value; n is the number of readings taken; $t_{\alpha}/2$ is the t value with $n - 1$ degrees of freedom, which can be obtained from the table of critical values of the student t distribution with specified confidence intervals and $n - 1$ degrees of freedom; and s

is the standard deviation for the experimental value. According to the student t distribution, the errors shown in Figures 5, 7, 8, 10, 11, and 15 were approximately 5%–8%, 4%–9%, 3%–6%, 3%–7%, 4%–8%, and 2%–4%, respectively.

CONCLUSIONS

Supramolecular magnetorheological polymer gels (SMRPGs) were synthesized by suspending iron particles in supramolecular polymer gels, which were suspended in *N*-octyl-pyrrolidone. The SMRPG network was obtained by metal coordination bonding between the functional group terpyridine and zinc ion. The results of this investigation indicate that the off-state viscosity of SMRPG can be controlled by adjusting the concentration of supramolecular polymer. The linear and nonlinear viscoelastic properties of SMRPGs under small- and large-amplitude oscillatory shear were investigated by using amplitude and frequency sweep mode. The effects of strain amplitude, frequency, and magnetic field strength on the viscoelastic moduli were investigated. Two methods were used to measure the settling behavior of SMRPG. Dynamic shear yield stress increased dramatically with the applied external magnetic field, and the settling rate decreased with an increase in supramolecular polymer concentration. These two measurements provided consistent results. It was observed that redispersion of MRPGs can be greatly improved by the incorporation of a supramolecular network into the SMRPGs.

References

1. Dang, A.; Liling, O.; Fales, J.; Stroeve, P. Ind Eng Chem Res 2000, 39, 2269.
2. Ginder, J. M. MRS Bull 1998, 26.
3. Phule, P.; Ginder, J. M. MRS Bull 1998, 19.
4. Wilson, M.; Fuchs, A.; Gordaninejad, F. J Appl Polym Sci 2002 84, 14, 2733.
5. Fuchs, A.; Gordaninejad, F.; Blattman, D.; Hamann, G. U.S. Pat. 6,525,972 (2003).
6. Fuchs, A.; Mei, X.; Gordaninejad, F.; Xiaojie, W.; Gregory, H.; Hatice, G.; Cahit, E.; George, K. J Appl Polym Sci 2004 92, 1176.
7. Brunsveld, L.; Folmer, B. J. B.; Meijer, E. W.; Silbesma, R. P. Chem Rev 2001, 101, 4071.
8. Ikkala, O.; Brinke, G. T. Chem Comm 2004, 19, 2131.
9. St. Pourcain, C. B.; Griffin, A. C. Macromolecules 1995, 28, 4116.
10. Manners, I. Science 2001, 294, 1664.
11. Kevin, J. C.; Gregory, N. T. Macromolecules 2002, 35, 6090.
12. Chujo, Y.; Sada, K.; Safgusa, T. Macromolecules 1993, 26, 6320.
13. Chujo, Y.; Sada, K.; Safgusa, T. Macromolecules 1993, 26, 6315.
14. Bas, G. G. L.; Helmut, S.; Ulrich, S. S. Macromol Symp 2003, 196, 125.
15. Harriman, A.; Ziessel, R. Chem Commun 1996, 7, 1707.
16. Potts, K. T.; Usifer, D. A. Macromolecules 1988, 21, 1985.
17. Jeffry, S. M. Curr Opin Colloid Interface Sci 1999, 4, 108.
18. Weihua, L. Ph.D. Dissertation, NanYang Technological University, 2000.
19. Gorodkin, S. R.; Kordonski, W. I.; Shorey, A. B.; Jacobs, S. D. Rev Sci Instr 2000, 71, 2476.
20. Munoz, B. C.; Adams, G. W.; Ngo, V. T.; Kitchin, J. R. U.S. Pat. 6,203,717 (1999).
21. Ulrich, S. S.; Christian, E. Macromol Symp 2001, 163, 177.
22. Ulrich, S.; Oliver, H.; Christian, E. Macromol Rapid Commun 2000, 21, 1156.
23. Gupta, R. K. Polymer and Composite Rheology; New York: L. E. Nielsen, 1977; Chapter 10.
24. Li, W. H.; Chen, G.; Yeo, S. H. Smart Mater Struct 1999, 8, 460.
25. Jong Heyok, P.; Moo Hyun, K.; Park, O. O. Korean J Chem 2001, 28, 580.
26. Byung Doo, C.; Jong Heyok, P.; Moo Hyun, K.; Park, O. O. Rheol Acta 2001, 40, 211.
27. Weihau, L.; Hejun, D.; Guang C.; Song, H. Y.; Ningqun, G. Rheol Acta 2003, 42, 280.
28. Seminar at the University of Nevada, Reno, NV, 2003.
29. Jolly, M. R. Mater Res Soc 2000, 604, 167.
30. Walpole, R. E.; Myers, R. H. Probability and statistics for engineers and Scientists, Macmillan: New York, 1978; Chapter 6.